Distribution Agreement

In presenting this thesis as a partial fulfillment of the requirements for a degree from Emory University, I hereby grant to Emory University and its agents the non-exclusive license to archive, make accessible, and display my thesis in whole or in part in all forms of media, now or hereafter now, including display on the World Wide Web. I understand that I may select some access restrictions as part of the online submission of this thesis. I retain all ownership rights to the copyright of the thesis. I also retain the right to use in future works (such as articles or books) all or part of this thesis.

Guoliang Zheng 04/02/2014

Aberrant Proteasome Pathway in Alzheimer's Disease at early stage revealed by whole-transcriptome study

By

Guoliang Zheng

Robert Cohen, MD, PhD

Adviser

Department of Neuroscience and Behavioral Biology

Paul Lennard, PhD

Committee Member

Darryl Neill, PhD

Committee Member

Aberrant Proteasome Pathway in Alzheimer's Disease at early stage revealed by whole-transcriptome study

By

Guoliang Zheng

Robert Cohen, MD, PhD

Adviser

An abstract of
a thesis submitted to the Faculty of Emory College of Arts and Sciences
of Emory University in partial fulfillment
of the requirements of the degree of
Bachelor of Sciences with Honors

Neuroscience and Behavioral Biology

2014

Abstract

Aberrant Proteasome Pathway in Alzheimer's Disease at early stage revealed by whole-transcriptome study

By Guoliang Zheng

Alzheimer's disease (AD) is characterized by extracellular amyloid plaques and intracellular neurofibrillary tangles. The major aim of the AD research is to identify biomarkers at the early stage of the disease to prevent it from progressing. The identification of these biomarkers can be explored through the determination of differential gene expression in the disease state and the normal state. The common platform for performing transcriptomes is cDNA microarray, however, it is associated with certain drawbacks. The development of high throughput mRNA-seq has been shown to resolve the issues related to microarray. Because transgenic AD rats at the two month age exhibit no amyloid plaques and behavioral impairment, which is equivalent to preclinical AD, we characterized the transcriptome of both AD and wild type (WT) rats at 2, 6, and 12 month to compare the level of gene expression, aiming to identify early pathogenic pathway that pertains to the late stage of AD through bioinformatics (DAVID) analysis. Because of the novelty of mRNA-seq, real time PCR was used for the validation of the mRNA-seq data. mRNA-seq reveals 2318 genes that exhibit consistent differential expression across the three ages, with 1587 genes downregulated, and 731 genes upregulated. DAVID identified the proteasome pathway that is mostly enriched in this gene set and four most significant proteasome associated genes were chosen for validation. Real time PCR results were in accordance with mRNA-seq results, indicating that the proteasome is affected in AD at early stage, and the mRNA-seq can be used for further investigation of other novel pathogenic pathways.

Aberrant Proteasome Pathway in Alzheimer's Disease at early stage revealed by whole-transcriptome study

By

Guoliang Zheng

Robert Cohen, MD, PhD

Adviser

A thesis submitted to the Faculty of Emory College of Arts and Sciences
of Emory University in partial fulfillment
of the requirements of the degree of
Bachelor of Sciences with Honors

Department of Neuroscience and Behavioral Biology

2014

Acknowledgements

I would like to acknowledge Dr. Cohen for his dedicated mentoring and guidance in my understanding of this devastating disease, and my involvement in this project; Dr. Smith for her thorough training on my lab skills, and my understanding of genetics, and her patience with me; Ogork for his direct assistance with my lab skills and project; Sophia for her guidance on certain lab procedures, and the genetics group in Cedar-Sinai medical center for their work on the mRNA-seq.

Table of Contents

Introduction

Pathogenesis

Alzheimer's Disease (AD) is known as the most common cause of senile dementia, with the number of Alzheimer's patients in the US estimated to reach 15 million by 2051 (Lopez, 2011). Although no physical alteration of brain is significant enough to serve as a diagnostic tool, hippocampal atrophy and symmetric lateral ventricle dilation offer reasonable clues for the diagnosis of AD (Perl, 2010). At the molecular level, AD is characterized by extracellular amyloid beta (Aβ) plaques (Masters et al., 1985) and intracellular neurofibrillary tangles (NFT) primarily formed by hyperphosphorylated tau proteins (Terry, 1963).

The most prominent hypothesis proposed for the pathogenesis of AD is that amyloid plaques trigger a cascade of events that lead to synaptic dysfunction and neuronal loss, known as amyloid cascade hypothesis (Selkoe, 2001). Briefly, a missense mutation in the Amyloid Precursor Protein *(APP),* Presenilin 1 (*PSEN1), or* Presenilin 2 (*PSEN2)* gene results in an abnormal proteolytic processing of APP at either the beta or gamma secretase site to generate an abnormal form of amyloid protein, the amyloid beta 42 (Aβ42) protein (Wildson et al., 1999). The Aβ42 proteins subsequently undergo oligomerization and fibrillization with the downstream effect of activating the immune systems in the central nervous system such as microglia that secrete cytokines and interleuckins, eventually leading to neuroinflammation (Mark, 2012; Gambi and Reale, 2009). NFTs that may be released following cell death have also been reported to have a progressive association with microglia activation (Sheng et al., 1997). In addition to the oligomerization, the Aβ42 proteins aggregate to form diffuse plaques. The

resulting neuritic injuries alter the ionic homeostasis and kinase activities and are speculated to be associated with the production of NFTs, and more widespread neuronal loss (Hardy and Selkoe, 2002).

However, there is a relatively weak association between the density of Aβ plaques and the severity of dementia (Ingelsson, 2004). Interestingly, there is a strong correlation between the NFT density and severity of dementia (Nagy et al., 1996). NFTs mainly consist of hyperphosphorylated tau proteins. Tau proteins bind to microtubules and are responsible for their stability. Abnormally phosphorylated tau proteins detach from microtubules, and disrupt axonal transport including that of intracellular organelles like mitochondria, eventually leading to mitochondria dysfunction and neuronal loss (Götz et al., 2004; Reddy, 2011). Additionally, increased oxidative stress has been proposed as an important pathogenetic component of AD upregulating Aβ42 production, and increasing, apoptosis of neurons through extrinsic and intrinsic pathways, and overactivating beta or gamma secretase (Cai et al, 2011).

Genetics and Disease models

The study of early onset familial AD cases has revealed three fully penetrant mutations: *APP*, *PSEN1*, and *PSEN2* (Tanzi and Bertram, 2001). In the light of these findings, genetically engineered mouse models have been developed expressing human APP PSEN1 and PSEN2 mutated proteins recapitulating AD-related phenotypes including behavioral impairment, Aβ deposition, mild tauopathy, neuroinflammation, and neuronal degeneration (Wong et al., 2002). However, these models have not been successful in reflecting the specifically robust tauopathy and neuronal loss of the human disease (Oddo et al, 2003). A new rat model TgF344-AD bearing mutant human *APP* and *PS1* does manifest the full spectrum of AD-related phenotypes including Aβ plaques, tau pathology, oligomeric Aβ protein,

memory deficits, and neuronal loss (Cohen et al., 2013). However, only 6-7% of the AD cases are categorized as early onset. Late-onset AD (LOAD) is governed by other genes with low penetrance in different loci (Avramopoulos, 2009). The APOE ε4 allele has been identified as the most important risk factor for LOAD with alleles in CLU, PICALM, CR1, BIN1, ABCA7, MS4A cluster, CD2AP, CD33, and EPHA1 identified in genome-wide association studies (GWAS) making smaller contributions (Harold et al., 2009, Lambert et al., 2009, Hollingworth et al., 2011). The discovery of these genetic risk factors assists in the identification of potential therapeutic targets.

An alternative to identifying therapeutic AD treatment targets through GWAS is to identify genes that are differentially expressed in the disease state. Using the hybridization based technique where mRNAs are first converted to fluorescently labeled complementary DNA (cDNA) and then hybridized to microarrays containing short oligomeric sequences, gene expression profiles have been established in the postmortem brains of both the early and the late onset patients, (Blalock et al., 2004; Liang et al., 2008; Ginsberg et al., 2000; Ricciarelli et al., 2004; Dunckley et al., 2006; Bossers et al., 2010) and of transgenic AD animal models (Reddy et al., 2004, Jee et al., 2005). Although this technique is high throughput and relatively inexpensive, there are limitations associated with it. First, it relies on the current knowledge of existing genome sequence. Second, there is the issue of "multiply targeted" probes that stems from cross hybridization yielding a false positive signal that can result in the unrelated probe sets appearing related (Okoniewski and Miller, 2006). Briefly, the optimal temperature dictating the binding of cDNA to the probes depends on the gene sequence, and the experiment is performed under one temperature. Therefore, the specificity of the binding is compromised and can result in the amplification of gene expression of low abundance transcripts (false positive signals). Lastly, comparing the data on gene expression levels from different microarray experiments remains a daunting task for researchers due to varying conditions of these experiments.

The development of Tag-based sequencing methods to study gene expression levels was intended as an alternative to hybridization approaches to correct many of these failings. In particular, sequencing methods resolve low false positive responses, demonstrate high reproducibility (Sultan et al., 2008; Tang et al., 2009), and can provide very precise and digital gene expression levels. For example, a previous study using Serial Analysis of Gene Expression profiled the transcriptome of the Tg2576-AD mouse model and found 6178 differential gene expressions between non-transgenic and Tg2576-AD mouse model (George et al., 2011). Using statistical analyses, they found clusters of altered gene expressions including downregulated G-protein-coupled receptor signaling, and odorant binding, yet upregulated cellular communication and cellular physiological processes. Despite the precise gene expression data, this technique is derived from the expensive Sanger sequencing technology, and gene isoforms are indistinguishable by this method (Wang et al., 2009).

Whole-transcriptome Technology

The development of whole transcriptome mRNA-Seq offers a rapid and thorough means to profile the transcriptome by analyzing the cDNA generated from the fragmented mRNA. The short reads (30 base pairs) provide information on the association of two exons, in contrast to multiple exons for long reads (Want et al., 2009). Thus, it provides the advantage of understanding the complex nature of eukaryotic organisms by identifying information on both exons and introns (Twine et al., 2011). In addition, using single-cell digital gene expression profiling assay helps to detect the expression of a greater number of genes than microarrasy techniques and as well as the ability to identify transcript variants at the whole-genome scale (Tang et al., 2009).

The identification of differential expressed genes in AD and wild type (WT) animal models can lead to the discovery of biomarkers. Therefore it was of interest to perform mRNA-seq in our AD rat models to discover potential biomarkers. In addition, it was considered important to discover preclinical biomarkers by performing mRNA-seq in AD rats at an age when little or no plaques and behavioral impairments are observable, as the ultimate goal of the research is to prevent the development of AD rather than face the daunting task of treating the disease. .

In this study, we use whole transcriptome mRNA-Seq to explore the differential gene expression of the *APP/PS1* mutant TgF344-AD rat and its littermate WT rat model. By clustering the genes that consistently exhibit differential gene expression in AD, when compared to WT, across 2, 6 (preclinical), and 12 (clinical) month old groups using bioinformatics tools, we could potentially identify the early pathogenic pathway, and discover the therapeutic targets that have the potential to be translated into the clinic. The mRNA-seq study identified 2318 genes that consistently exhibited differential expression across the 2, 6, and 12 months age, with 1587 genes upregulated, and 731 downregulated. From the bioinformatics analysis, the genes associated with the proteasome pathway are considered to be the most overrepresented and significant among the 34 pathways identified. Four genes considered to be most closely associated with the proteasome were selected for real time PCR validation. The data generated provide support for the initial illumina RNA-seq findings.

Methods

Samples and mRNA sequencing

The mRNA sequencing and data analysis was performed by the genetics group in Cedar-Sinai Medical Center in Los Angeles. Two, six, and twelve months old TgF344-AD rats with "Swedish" mutant human APP (APP_{SW}) and Δ exon 9 mutant human presenilin-1 (PS1ΔE9) genes (n=5 per group) and wild type rats of equivalent age (n=5 per group) were euthanized and RNA extracted from whole brains. The ages of the groups chosen for this experiment correspond to the different clinical stages of AD. The two month old rats manifest no Aβ plaques and no behavioral impairment, representing the preclinical stage of AD; the six month old rats manifest a moderate amount of diffuse Aβ plaques and no behavioral impairment, representing a transition stage between preclinical and clinical AD, perhaps equivalent to the human condition of early mild cognitive impairment (MCI); the 12 month old rats manifest global neuritic plaques, and behavioral impairments, representing ADTo reduce cost, 10 μg of total RNA derived from each animal was pooled to create 6 samples (2 mo. AD, 2 mo. WT, 6 mo. AD, 6 mo. WT, 12 mo. AD, 12 mo. WT) for sequencing. The quality of each pooled RNA sample was evaluated using the Agilent 2100 Bioanalyser RNA Nano Chip, and met the standard cutoff set by Illumina (>8). Because mRNA contains poly A tail at the 3 prime end, a Sera-Mag magnetic oligo bead with poly T was used to purify the mRNA from the 2 μg total RNA of each pooled sample. Large RNA molecules must be fragmented to 200-500 bp to accommodate the deep-sequencing technologies. Therefore after purification, mRNA was fragmented at a high temperature using divalent cations. The fragmented mRNA was converted to the first strand cDNA using Super-Script II reverse transcriptase and random primers. The second strand was generated with the first strand as the template using DNA polymerase IKlenow fragment, T4 polynucleotide kinase and T4 polymerase, were used to remove and convert 3 prime end

overhangs, the result of imperfect second strand synthesis, into blunt ends. For the adapters with the single T base to recognize and bind to the cDNA, an A base was added to the 3 prime end using Klenow fragment to adenylate it. 50ml, 2% agarose gel was used to perform size selection (200-250bp) for cDNA library construction and the selected band on the gel was isolated for downstream amplification. The cDNA library was enriched using polymerase chain reaction (PCR) for 15 cycles. Finally, the library was subjected to a quality analysis using Agilent Technologies 2100 Bioanalyser with a DNA specific chip. After quality control, each library (6 libraries are generated) was sequenced on one Genome Analyzer (GAII) lane with 36-bp sequencing. Sequencing was accomplished through synthesis by taking advantage of a proprietary method of detecting single bases as they are incorporated into growing DNA strands.

Gene Mapping and Transcripts Assembling

An individual library was created for each of the 6 pooled RNA samples. The preliminary reads from the 6 libraries were obtained from the Illumina machine Bustard. Six FASTQ files were generated for quality control. No (0) or yes (1) was used as the standard for whether the reads passed the filtering process. The processed reads were aligned to the rat reference genome obtained from USCS with TopHat. TopHat utilizes Bowtie, an efficient read alignment program to complete the initial screening and mapping, and estimates the junction's splice sites that the Bowtie fail to align the reads onto. The splice variants (isoforms) identification relies on the current knowledge of isoforms of certain genes, and the limitation on the isoform annotations can result in inaccurate determination of expression level. The use of the Cufflinks package can potentially solve this problem by inferring the splice variants numbers and structures. Cufflinks was used to determine the abundance of each transcript by first assembling the reads to transcripts. The transcript abundance of the genes was then measured in Fragments Per Kilobase of exon per million fragments mapped (FPKM) (Mortazavi et al., 2008). Sequence alignment

data were stored in BAM (bam) and SAM (.sam) files. A BAM file is the binary version of a SAM file that includes sequencing alignment data. The assembled transcripts were subjected to Cuffdiff for statistical analysis to determine the statistically differentially expressed transcripts in the two conditions (AD vs. WT) based on the assumption that the gene expression level is proportional to the abundance of transcripts. Student t-tests were used to detect the genes that were consistently differentially expressed between the transgenic and WT animal models across the 2, 6, 12 months groups with a cutoff p-value $10^{-5}$to adjust for multiple comparisons.

Gene ontology enrichment analysis

The Database for Annotation, Visualization, and Integrated Discovery (DAVID) bioinformatics tool was used to map the large volume data generated from high throughput methods to the associated annotation (e.g., gene ontology), and to select the gene sets enriched for specified biological processes (Huang et al., 2008). In particular, the DAVID gene functional classification allows investigators to explore functionally related genes as a group rather than at the individual level. We input the gene lists generated from the above mRNA-seq data analysis, converting the gene IDs to symbols that DAVID could recognize, and utilized the gene functional classification to visualize the functional groups with a tubular view. Subsequently, a subgene list was generated based on the enrichment score reported by the gene functional classification algorithm. Enrichment score is a parameter used to determine the extent of a certain gene set is overrepresented and not likely chosen by random.

Real-Time PCR (qPCR): Gene expression validation

Four genes with the highest kappa values were selected from the most enriched gene clusters identified using DAVID. The kappa values measure the degree of agreement between genes with respect to their proposed parts in specific biological processes. The use of housekeeping genes that are stably expressed in all cells contributes to data normalization to compensate for sample-to-sample or run-to-run variations, thus decreasing error. (Pfaffl and Hagele, 2001). To qualify as housekeeping genes for this study, it was important to establish that a candidate gene had to show equal expression in both AD and WT animals at the three ages selected for study. A pilot study was carried out to determine the housekeeping gene to be used in our qPCR for data normalization. An excel file containing a broad list of housekeeping genes recommended for qPCR was used to compare to our list containing genes with comparable expression level in transgenic and WT animals across the three different age groups (Eisenberg and Levanon, 2013). 31 genes met the criteria for data normalization. We picked three genes associated with protein processing (*Gga1*), metabolism (*Atp6v0c*), and vesicle transport (*Cltb*) for our pilot study. RNA was extracted from WT and AD animal brains using the Agilent RNA extraction kit (Agilent Technologies, USA), and the concentration of the RNA was determined using Nanodrop. The total RNA was converted to cDNA using a high-capacity reverse transcription kit (Applied Biosystem Techonologies, USA), and the concentration of the cDNA was determined using Nanodrop. The cDNA concentration was diluted to a preset concentration (i.e. 10ng/µl) as the template, and mixed with target gene assay and Taqman gene expression master mixes in preparation for qPCR. The number of cDNA amplification cycles required before a detectable fluorescent signal was observed (Ct or threshold cycle) and used as a measure of mRNA concentration.

Once a useful housekeeping gene was determined, the 30 RNA samples used for the mRNA-seq were converted to cDNA samples for the qPCR. These 30 cDNA samples were normalized to similar

concentrations (i.e. 10ng/µl), and were buffered with gene expression assays and master mix and placed onto four 384 well cDNA plates (each for different target genes respectively). The plates were structured for three measures of each target and housekeeping gene on each individual animal sample. Two water samples were added as negative controls for a total of 204 reactions for each plate. The C_t values computed by the qPCR were obtained and the delta C_ts were calculated by subtracting the average C_t values of the housekeeping gene (*Cltb*) from the average C_t values of each of the each target genes. These C_t values are grouped into 6 groups for each target gene based on age and disease (or genotype) state (i.e. two month AD), and an overall ANOVAR (repeated measures analysis of variance) was conducted to evaluate to determine an overall statistical significance of proteasome gene expression differences.

Results

Differentially Expressed Genes

Two BAM files were obtained for each pooled sample, one containing known gene transcript data, and the other containing unknown gene transcript data. In the BAM files containing known gene transcripts, 17,133 gene isoforms were identified, and approximately 2318 genes were differentially expressed in the same direction between AD and WT rats reaching statistical significance at all 3 ages ($p<10^{-5}$). 1587 genes were downregulated, and 731 genes were upregulated in the AD rats compared to their WT littermates. The predominant downregulation indicates a decreased transcriptional activity in the AD rats when compared to the WT rats. Interestingly, we observed many zero reads among the downregulated gene list. Most of these genes had very low, but discernible read counts (<1) in WT animals. When comparing the gene list from mRNA-seq to previous microarrays experiments (Blaolock

et al., 2004), we observed some concordance in gene expression differences, with 48 genes upregulated in the rats also being upregulated in postmortem AD hippocampus, and 48 genes downregulated in the rats also having previously been reported to being downregulated in postmortem AD hippocampus. The genes encoding ribosomal protein predominate the population of genes up-regulated in both rats and humans, with the most closely related to the ribosomal pathway being*, RPL18, RPLP0, RPS11 RPL4, RPS9, RPL11* (Table 1, Kappa value=0.87, 0.81. 0.79, 0.79, 0.71, 0.58). Kappa value is a statistic parameter that measures the strength of association between two parameters, in this case, the genes and the ribosomal pathway. However, no common pathway is identified statistically significant for the genes identified as down-regulated in both rat and human postmortem brain. The most representative genes (i.e. the most down-regulated) include heat shock protein 8 (*Hsp8*), synaptogyrin 1(*Syngr1*), Neurogranin (*Nrgn*), Cyclin-dependent kinase 5 (*Cdk5r2*), and cholecystokinin (*Cck*).

Gene Ontology term enrichment analysis

DAVID was used to identify functional association in the genes that are differentially expressed. Rather than inputting the downregulated and upregulated gene lists separately, the whole gene list was subjected to DAVID analysis because genes might be both upregulated and downregulated in a common pathway. The gene cluster with the highest enrichment score (ES) was that of the proteasome (Table 2, ES=7.97). The other clusters that are also significantly enriched are the genes associated with the ubiquitin system (ES= 6.98), the ATPase system (ES= 6.65), the ribosomal protein system (ES=5.59), and mitochondria system (ES=4.8). These systems have been previously implicated in the pathogenesis of AD. As the proteasome pathway was found to be the most enriched, genes from this cluster were chosen to verify the mRNA-seq data by qPCR. The qPCR was not conducted with the most upregulated (the highest fold change in gene expression) or downregulated because these genes, while statistically

significant, may not prove to be as biologically significant. Within the gene cluster associated with the proteasome pathway, the gene with the highest Kappa value (KV) was the proteasome 26S subunit, non-ATPase, 14 (Psmd14, KV=0.93). The majority of the genes within this gene clusters are associated with the proteasome 26S subunit. KV is a statistic parameter that defines the strength of inter-relationship of two subjects, in this case, the gene and the proteasome. Four genes with high KVs were chosen for our initial qPCR confirmatory analysis: Psmd14, Psmd6 (Table 3, KV=0.91),), Psma5 (KV=0.87), and Psmb1 (KV=0.87).,

Real Time PCR analysis

The concentration of cDNA is proportionally related to the gene expression level and thus is an indicator of the gene expression level. The relative concentration of cDNA level is approximated by the delta C_T (target gene C_T - C_T of the reference (housekeeping) gene. For a prominent housekeeping gene, it should not vary by biological conditions, and should have a comparable C_T value under different biological conditions. Of three possible candidate housekeeping, the delta C_T of *Cltb* is the smallest (2) when compared to the other two genes (4.2, 3.8). Therefore, *Cltb* was used as the housekeeping gene for the normalization of the experiment.

An initial ANOVAR was performed to evaluate the main effects of AGE (levels = 2, 6, 12) and GENOTYPE (levels = WT, AD) and GENE (levels = PSMA5, PSMD6, PSMB1, PSMB14) the possible interaction terms of AGE x GENOTYPE, AGE x GENE, GENE x GENOTYPE and AGE x GENOTYPE x GENE on the expression levels of the 4 chosen proteasome genes as a whole. No statistically significant interaction terms were found. Main effects were observed for GENOTYPE (AD > WT, $p = .006$) and for GENE ($p < 10E-6$), but not for AGE (see Table 4). The results indicate that there is significant difference

of gene expression level in AD and WT, and no significant difference occurs across different age groups. Additionally, the difference in AD and WT does not depend on age. Thus overall, the qPCR data are in accordance with the mRNA-seq data that an upregulation of proteasome mRNA occurs in the AD. The fold change of gene expression is calculated by taking the exponential of delta CT to reflect the initial concentration ratio of AD to WT. The fold change calculated with qPCR data is 2.8, 1.7, 2.7, and 2.5 for *Psmd14, Psma5, Psmd6, Psmb1* respectively, indicating an overall upregulation in AD when compared to WT (Table 5). The fold change calculated with mRNA-seq is 4.4, 3.8, 3.7 and 2.7 for *Psmd14, Psma5, Psmd6, Psmb1* respectively, indicating the real time PCR data of these genes follow the same trend in the mRNA-seq data.

Discussion

mRNA-seq

This study provides comprehensive information on the whole transcriptome of the transgenic AD (TgF-344) rat brain using a relatively novel technology mRNA-seq. cDNA microarray has been used predominantly in the past for the determination of gene expression level, and is considered as the "gold standard" of such experiments. However, cDNA microarray has its inherent limitations, resulting in compromised accuracy of determination of gene expression levels. The issues associated with the cDNA microarray is that the probe sometimes accidentally hybridize to the background, making the detected expression level higher than the actual expression level (false positive signal), especially for the transcripts at low abundance. In addition, mRNAs-seq does not depend on the current knowledge of genomics, and can actually expand on it by detecting novel gene isoforms, and accurately detect the transcripts at low abundance, that tend to be amplified beyond the actual expression level. An mRNA-

seq using single mouse blastomere has detected 5270 (75%) more genes than when using microarray (Tang et al., 2009). In addition, it has identified 1753 unknown splice junctions, demonstrating the complexity of the transcript variants at whole-genome scale.

mRNA-seq has been done in the AD field on the brain tissues derived from frontal lobe, temporal lobe, and whole brain of the postmortem AD patients, and has demonstrated a robust experimental design in conducting the mRNA-seq (Twine et al., 2011). Despite the introduction of mRNA-seq to the AD field and the strong experimental design, the results have not provided novel insights into the primary pathogenic mechanisms of AD. Because extensive neuronal degeneration at the late stages of AD, the use of postmortem brain in conducting mRNA-seq might primarily yield insights into the inflammatory changes or compensatory mechanisms that are occurring at this late stage of the illness rather than the initiating events that are most important for the development of targeted therapies (Sutherland et al., 2011) directed to prevention or early treatment or for the development of biomarkers for these same states. The use of brain tissues from transgenic animal models at ages that precede the onset of behavioral impairment and plaque deposition is one important approach that can meet this need. Our inclusion of 2 and 6 months old transgenic rat models having no or some diffuse plaques and the absence of behavioral impairment (Cohen et al., 2013) renders the study the confidence in identifying the early pathogenic mechanisms, and potentially future therapeutic targets. The other issue associated with postmortem brain is that the cause of death of AD patients varies greatly among patients, with 35% of patients dying of bronchopneumonia (Molsa et al., 1986), Variation among agonal states and preceding medical conditions, postmortem interval and postmortem variation in preservation in addition to variation in genetic makeup among humans are likely to reduce the power for detecting disease specific changes in the transcriptome. Our rat brains are collected and stored at -80°c after perfusion, and the RNA extraction is performed in a timely fashion. Because the

hippocampus and the entorhinal cortex are often the most vulnerable brain regions to AD at the early stage (Gomez-Isla et al., 1996), whole-brain transcriptome may have masked the information yielded specifically from these regions. Thus, it would of interest to perform mRNA-seq in the brain tissues derived from these two regions of the rat models, and compare the data to this study to determine if there are different mechanisms involved in the early pathogenesis. Although these concerns are somewhat offset by the fact that transgene expression occurs throughout the rat brain, the relative large size of the hippocampus to the rest of the brain in the rat and the sensitivity of RNA-seq data, thus allowing for the determination of mRNAs that may be primarily expressed in only a few regions.

Interestingly, in our downregulated gene lists, the majority of transcripts of the AD rat models have zero read counts (no gene expression), and the majority of transcripts of the WT rat models have read counts <1 (very low gene expression). These transcripts are termed as rare transcripts, and they are found in many cells, whereas the exact function of these rare transcripts remains unknown. Usually these rare transcripts are expressed in the cells that have no seemingly functional association to these transcripts (maybe include a reference). One of hypothesis could be that the expression of these rare transcripts is an evolutionary adaptation response to the rapid changing environment to help the cell to survive. These transcripts could regulate the transcription process to produce proteins that are critical for the survival of cells at this time. If the genes actually have no expression and the hypothesis holds true, the implication for AD is that the neurons affected by AD are no longer capable of triggering the evolutionary mechanism necessary for the survival of these neurons, and further allows the progression of AD to take place. However, the zero read counts could also be result of transgene interruption, which is not very likely because there are some genes not affected. Thus it is of interest to determine whether there is actually no expression in the AD state by performing a qPCR to validate the findings from mRNA-seq. If the results from qPCR agree with the results from mRNA-seq, the hypothesis can be tested by

measuring the response of cells, with a knock out of certain gene encodes for rare transcripts, and normal cells to a harsh environment, and determine whether the normal cells with the rare transcripts can survive.

The Ubiquitin-Proteasome System

The functional classification tool of DAVID identifies 34 gene clusters with the highest classification stringency (cutoff for ES is 0.1). The most enriched gene cluster is associated with the proteasome pathway. The ubiquitin-proteasome system (UPS) is mainly responsible for degrading the intracellular proteins through a series of complex regulated process. The degradation of intracellular proteins usually involves the binding of the ubiquitin to the substrate generating a proteolytic signal to the proteasome, and proteasome 26S subunit recognizes the signal as an indication to degrade the tagged protein, while recycling the ubiquitin for another cycle of protein degradation (Ciechanover and Brundin, 2003). Because the protein degradation process is critical in the cellular process, any aberrations could lead to pathogenesis.

Although the major hallmark of AD is the extracellular amyloid plaque, the clinical trials intending to treat AD by targeting the Aβ plaque with immunotherapy have largely failed (Castillo-Carranza et al., 2013). There is increasing evidence that intracellular Aβ accumulation may play a more important or at least complementary role to extracellular Aβ role in the pathogenesis of AD (Hong et al., 2014). Aberrant accumulation of intracellular Aβ has been observed in the pyramidal neurons of the hippocampus and entorhinal cortex before the extracellular amyloid plaques are observed (Watanabe et al., 2012). This finding has directed attention to the UPS and how it may fail to prevent the accumulation of Aβ. The degradation of Aβ42 in cultured cortical neurons is significantly decreased after the proteasome is inhibited by lactacystin, suggesting that the Aβ42 is

a substrate of the UPS of neurons (Lopez et al., 2003). Thus aberrant accumulation of intracellular Aβ42 as observed in early AD might signal the dysfunction of the UPS as a triggering event in AD that subsequently leads to amyloid plaques. In addition, the aggregation of the hyperphosphorylated tau proteins inside the cell, leading to the formation of NFT, may also be the result of said dysfunction although the exact mechanisms whereby this might occur remains unknown. How might UPS dysfunction develop? Studies have suggested that Aβ itself might be the causative agent (Lopez et al., 2003; Almeida et al., 2006). For example, several studies suggest that Aβ is responsible for the inhibition of the proteasome by occuping the 20s subunit of the proteasome (responsible for proteolytic activity) and also by inhibiting the beta5 chymotrypsin-like activity (Gregori et al., 1997; Zhao and Yang, 2010). Additional evidences supporting the inhibition of the proteasome by Aβ derives from the observed reduction of proteasome activity in postmortem brain of AD patients (Keller et al., 2000). The reduction is observed in the vulnerable brain regions including the hippocampus and the entorhinal cortex, but is spared in the occipital lobe and the cerebellum areas known to be relatively free of AD pathology in all but the latest stages of the disease. Additionally, NFT have been demonstrated to coimmunoprecipitate with proteasome subunits and inhibt their function (Keck et al., 2003). Thus the two hallmarks of AD are found physically associated with proteosomes and can both induce proteasome dysfunction suggesting an important role of the proteasome in the pathogenesis of AD.

The other evidence suggesting the role of proteasomes in the pathogenesis of AD is the discovery of a mutation of ubiquitin (UBB^{+1}) at the transcriptional level, leading to a deletion of the C-terminal end of ubiquitin (van Leeuwen et al., 2000). The deletion results in a ubiquitin that can no longer tag proteins for degradation, and instead being ubiquinated by the normal ubiquitin forms a polyubiquinated ubiquitin, which the proteasome fails to degrade. The result is the inhibition of the proteasome 26S subunit (Hope et al., 2003). Elevated UBB^{+1} is observed in the

neurons of AD patients as well as patients of other neurodegenerative diseases (val leeuwen et al., 1998). Further, overexpression of UBB^{+1} *in vitro* inhibits the proteasome (De Vrij et al., 2001). Although it is not likely that mutations of ubiquitin are important causative factors in AD, these findings contribute to circumstantial data supporting an important role of ubiquitin dysfunction in the pathogenesis of AD. Whether the reduction of proteasome activity results in more accumulation of Aβ or the Aβ accumulation inhibits the proteasome from degrading them is not clear, but what is clear is that it is likely that once Aβ begins to accumulate that proteasomes are part of an unfortunate feed-forward system that contributes to ever increasing levels of Aβ.

Interestingly, the expression level of the genes associated with the proteasome pathway output by the DAVID bioinformatics increases in the AD state when compared to the normal state. It seems contradictory to the observed reduction of proteasome activity in the neurons of AD patients. One explanation is that this is likely a compensatory mechanism by enhancing the expression level of the genes associated with the proteasome pathway to compensate for the inhibition of proteasome, and thus prolonging the survival of affected neurons. For example, the inhibition of cell proteasome function with proteasome inhibitors induces an upregulation of all mammalian 26S proteasome subunit mRNAs (Meiners et al., 2003). As a result, the synthesis of de novo proteins and proteasomes are greatly elevated in response to the proteasome inhibition, confirming the upregulated genes can be a compensatory mechanism in response to cell damage.. However, whether the upregulation of transcripts associated with proteasome pathway produces more proteins and proteasomes remains to be confirmed. Western blots could be used to determine whether the level of the proteins encoded by the upregulated transcripts observed in our current work are increased. If the results demonstrate such an increase, then it is possible that an overactive proteasome might be playing a role in degrading essential proteins thus worsening the condition of neurons in AD.

With the accumulation and misfolding of intracellular Aβ due to the inhibition of proteasome, a cellular mechanism termed unfolded protein response (UPR) is triggered to protect the neuron from the build up of toxic Aβ (Hoozemans et al., 2009). When the protein misfolds, endoplasmic reticulum (ER) chaperones BiP/GRP78 bind to the other three proteins including pancreatic ER kinases (PERK), transcription factor ATF-6, and endoribonuclease IRE-1 to activate them (Harding et al., 1999). Once the UPR is activated, translation decreases, and the production of the ER chaperone increases to assist in protein folding (Kozutsumi et al., 1998). Western blot analysis reveals that the level of ER chaperones increases in the AD hippocampus when compared to the control, indicating the activation of UPR in the AD. Additionally, the phosphorylated PERK is observed in AD patients but not in non-demented controls (Hoozemans et al., 2005). The occurrence of UPR in the neurons without other apparent AD pathological features suggests its involvement in the early stage of AD. Interestingly, our study intending to assess the early pathogenic mechanisms of AD reveals the involvement of the aberrant proteasome pathway in AD.

How might this all play out? Mildly elevated levels of Aβ would be expected to inhibit proteasome function leading to elevated proteosomal pathway mRNA in an attempt to compensate for the reduction of proteasome activity. Inadequate compensation would be expected to induce a UPR response to assist the folding of Aβ. Although the UPR activation is in an attempt to protect the neurons from the toxic effect of misfolded Aβ accumulation, the constant activation may initiate the progression of the disease. When facing acute stress, the cell responds with translational repression and it proves to be protective. However, in AD with chronic stress, the UPR is constitutively activated, ceasing the production of essential proteins for the cell survival.

Therapeutic targets can be developed based on the paradigm discussed above by targeting the intracellular Aβ to release the inhibition of proteasome pathway for the clearance of Aβ. The applicability of this therapy requires the knowledge of the type of Aβ that is inhibiting the

proteasome. The immunotherapy against the Aβ oligomers, rather than the monomers, in the 3xTg-AD mouse models rescues the proteasome, and thus improve the cognitive function of these mice (Tseng et al., 2007). Additionally, pharmaceuticals attempting to activate the proteasome pathway can be developed to enhance the proteasome activity in the AD population. Lastly, pharmaceuticals aiming to balance the restoration of translation for essential proteins, and the repression of translation for misfolded proteins could be developed to treat AD (Halliday et al., 2014).

Tables and Figures

Enrichment Score: 4.4308

Gene Symbol	Gene Name	Kappa Value
Rpl18	Ribosomal Protein L18	0.87
Rps11	Ribosomal Protein S11	0.81
Rplp0	Ribosomal protein, Large P0	0.79
Rpl4	Ribosomal protein L4	0.79
Rps9	Ribosomal Protein S9	0.71
Rpl11	Ribosomal Protein L11	0.58

Table 1. DAVID Gene cluster associated with ribosome pathway

Gene Cluster	Enrichment Score	Pathway Affected
1.	7.97	Proteasome
2.	6.98	Ubiquitin
3.	6.96	ATPase
4.	5.62	NADH dyhydrogenase
5.	5.59	Ribosomal Protein
6.	4.65	Ubiquitin-cytochrome
7.	3.87	Ubiquitin Specific Peptidase
8.	3.56	Coatomer protein complex
9.	3.45	RAS oncogene family
10.	3.43	GTPase
11.	2.51	Kinesin family
12.	2.44	Mitochondrial carrier
13.	2.39	ATP-binding cassette
14.	2.36	RT1 class
15.	2.17	tRNA-synthetase
16.	2.14	Polypyrimidine tract binding protein 2

17.	1.8	Kinase family
18.	1.62	Nucleosome assembly protein
19.	1.52	Coiled-coil domain containing 104
20.	1.24	Glutamate receptor

Table 2 Top 20 gene clusters identified with DAVID bioinformatics tool

Enrichment Score: 7.97

Gene Symbol	Gene Name	Kappa Value
Psmd14	Proteasome 26S subunit, non-ATPase, 14	0.93
Psmd6	Proteasome 26S subunit, non-ATPase, 6	0.91
Psma5	Proteasome 26S subunit, non-ATPase, 12	0.91
Psmb1	Proteasome subunit, alpha type 5	0.87
Psma4	Proteasome subunit, beta type 1	0.87
Psma2	Proteasome subunit, alpha type 4	0.86

Psma1	Proteasome subunit, alpha type 2	0.86
Psme2	Proteasome subunit, alpha type 1	0.85
Psme1	Proteasome activator subunit 2	0.85
Psma3	Proteasome activator subunit 1	0.85
Psma6	Proteasome subunit, alpha type 3	0.84
Psmd2	Proteasome subunit, alpha type 6	0.84
Psmb6	Proteasome 26S subunit, non-ATPase, 2	0.83
Psmc2	Proteasome subunit, beta type 6	0.82
Psmd10	Proteasome 26S subunit, ATPase2	0.82
Psmb9	Proteasome 26S subunit, non-ATPase, 10	0.81
Psmd1	Proteasome subunit, beta type 9	0.81
Psmc6	Proteasome 26S subunit, non-ATPase, 1	0.80
Psmb8	Proteasome 26S subunit, ATPase6	0.79
Psmc1	Proteasome subunit, beta type 8	0.79
Psmb4	Proteasome 26S subunit, ATPase1	0.78
Psmc5	Proteasome subunit, beta type 4	0.76
Anapc5	Proteasome 26S subunit, ATPase5	0.74

Ubb	Anaphase-promoting complex subunit 5	0.72
Fzr1	Ubiquitin C, B	0.57
Cul1	Fizzy/cell division cycle 20 related 1	0.57
Ufd1l	Cullin 1	0.55
	Ubiquitin fusion degradation 1 like	0.43

Table 3. DAVID gene cluster associated with proteasome pathway

1=GENOTYPE 2= AGE 3=GENE	df Effect	MS Effect	df Error	MS Error	F	p-level
1	1	25	17	2.66	9.7	0.006
2	2	4.2	17	2.66	1.6	0.23
3	3	61	51	1.51	40.	1.9E-13
12	2	4.5	17	2.66	1.7	0.21
13	3	0.8	51	1.51	0.52	0.67
23	6	1.7	51	1.51	1.1	0.36
123	6	2.0	51	1.51	1.3	0.26

Table 4. ANOVAR on GENOTYPE, AGE, and GENE

Gene Name	qPCR fold change	mRNA-seq fold change
Psmd14	2.8	4.4
Psmb1	2.5	2.7
Psma5	1.7	3.8
Psmd6	2.7	3.7

Table 5 Comparison of normalized fold changes for RT-PCR and mRNA-seq

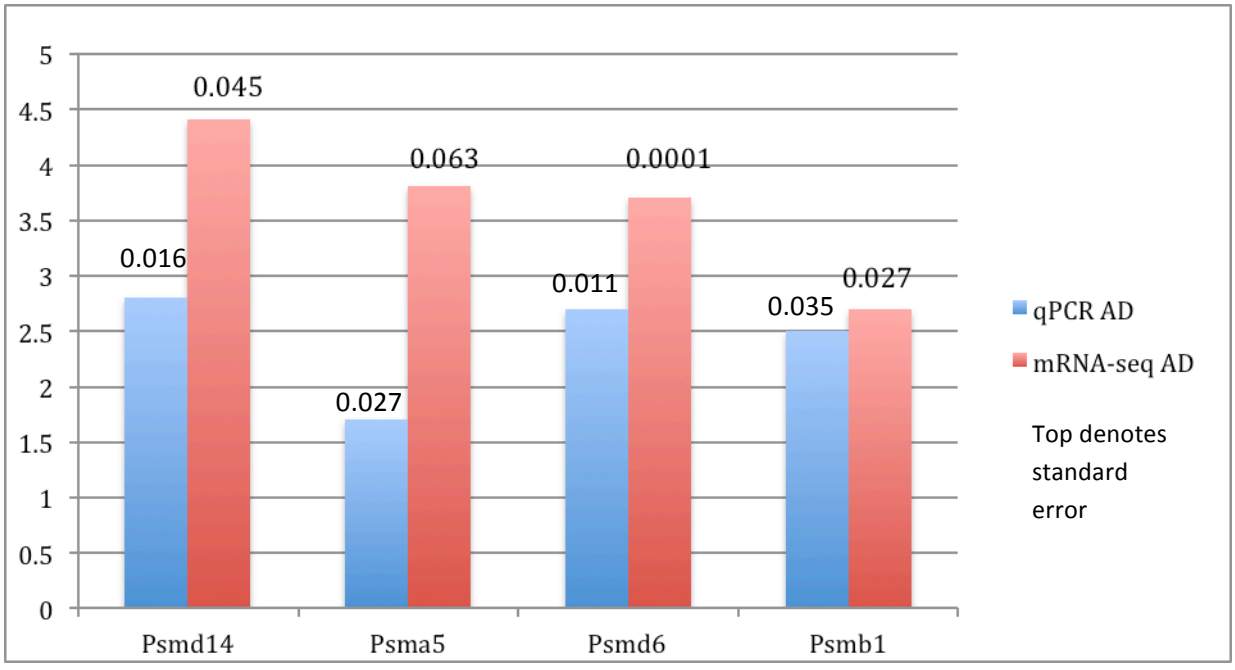

Fig 1 RT-PCR validation of selected genes and comparison to mRNA-seq

References:

1. Almeida CG, Takahashi RH, Gouras GK (2006) Beta-amyloid accumulation impairs multivesicular body sorting by inhibiting the ubiquitin-proteasome system. J Neurosci. 26:4277-88

2. Avramopoulos D (2009) Genetics of Alzheimer's disease: recent advances. Genome Med 1,34

3. Blalock EM, Geddes JW, Chen KC, Porter NM, Markesbery WR, Landfield PW (2004) Incipient Alzheimer's disease: microarray correlation analyses reveal major transcriptional and tumor suppressor responses. Proc Natl Acad Sci USA 101: 2173-2178

4. Bossers K, Wirz KT, Meerhoff GF, Essing AH, van Dongen JW, Houba P, Kruse C, Verhaagen J, Swabb DF (2010) Concerted changes in transcripts in the prefrontal cortex precede neuropathology in Alzheimer's disease. Brain 133: 3699-3723

5. Castillo-Carranza DL, Guerrero-Munoz MJ, Kayed R (2013) Immunotherapy for the treatment of Alzheimer's disease: amyloid-β or tau, which is the right target? Dovepress

6. Cai Z, Zhao B, Ratka A (2011) Oxidative Stress and β-Amyloid Protein in Alzheimer's disease. Neuromol Med 13: 223-250

7. Ciechanover A, Brundin P (2003) The Ubiquitin Proteasome System in Neurodegenerative Diseases: Sometimes the Chicken, sometimes the Egg. Neuron 40: 427-446

8. Cohen RM, Rezai-Zadeh K, Weitz TM, Rentsendorj A, Gate D, Spivak I, Bholat Y, Vasilevko V, Glabe CG, Berunig JJ, Rakic P, Davtyan H, Agadjanyan MG, Kepe V, Barrio JR, Bannykh S, Szekely CA, Pechnick RN, Town T (2013) A Transgenic Alzheimer Rat with Plaques, Tau Pathology, Behavioral Impairment, Oligomeric Aβ, and Frank Neuronal Loss. J Neurosci 33(15): 6245-6256

9. Coon KD, Myers AJ, Craig DW, Webster JA, Pearson JV, Lince DH, Zismann VL, Beach TG, Leugn D, Bryden L, Halperin RF, Marlowe L, Kaleem M, Walker DG, Ravid R, Heward CB, Rogers J, Papassotiropoulos A, Reiman EM, Hardy J, Stephan DA (2007) A high-density whole-genome association study reveals that APOE is the major susceptibility gene for sporadic late-onset Alzheimer's Disease. J. Clin. Psychiatry 68, 613-618.

10. De Vrij FM, Slujis JA, Gregori L, Fischer DF, Hermens WT, Goldgaber D, Verhaagen J, Van Leeuwen FW, Hol EM (2001) Mutant ubiquitin expressed in Alzheimer's disease causes neuronal death. FASEB J, 15: 2680-2688

11. Dunckley T, Beach TG, Ramsey KE, Grover A, Mastroeni D, Walker DG, LaFleur BJ, Coon KD, Brown KM, Caselli R, Kukull W, Higdon R, Mckeel D, Morris JC, Hulette C, Schemechel D, Reiman EM, Rogers J, Stephan DA (2006) Gene expression correlates of neurofibrillary tangles in Alzheimer's disease. Neurobiol Aging 27:1359-1371

12. Eisenberg E, Levanon EY (2013) Human housekeeping genes, revisited. Trends in Genetics

13. Gambi D, Reale M (2009) A Pathophysiological Role for Selective Alteration of the Cytokine-Chemokine Network- Inflammatory Theory in Alzheimer's disease. European Neurological Review, 22-24

14. George AJ, Gordon L, Beissbarth T, Koukoulas I, Holsinger RM, Perreau V, Cappai R, Tan SS, Masters CL, Scott HS, Li QX (2010) A Serial Analysis of Gene Expression Profile of the Alzheimer's Disease Tg2576 Mouse Model. Neurotox Res 17: 360-379

15. Ginsberg SD, Hemby SE, Lee VM, Eberwine JH, Trojanowski JQ (2000) Expression profile of transcripts in Alzheimer's disease tangle-bearing CA1 neurons. Ann Neurol 48:77-87

16. Gomez-Isla T, Price JL, Mckeel DW, Morris JC, Growdon JH, Hyman BT (1996) Profound loss of layer II entorhinal cortex neurons occurs in very mild Alzheimer's disease. J. Neurosci, 16: 4491-4500

17. Götz J, Schild A, Hoerndli F, Pennanen L (2004) Amyloid-induced neurofibrillary tangle formation in Alzheimer's disease: insight from transgenic mouse and tissue-culture models. Int. J. Dev. Neurosci 22: 453-465

18. Gregori L, Hainfeld JF, Simon MN, Goldgaber D (1997) Binding of amyloid beta protein to the 20S proteasome. J Biol Chem, 272: 58-62

19. Halliday M, Mallucci GR (2014) Targeting the unfolded protein response in neurodegeneration : A new approach to therapy. Neuropharmacology, 76: 169-174

20. Hardy J, Selkoe DJ (2002) The Amyloid Hypothesis of Alzheimer's disease: Progress and Problems on the Road to Therapeutics. Science 297, 353

21. Harding HP, Zhang Y, Ron D (1999) Protein translation and folding are coupled by an endoplasmic-reticulum-resident kinase. Nature, 397: 271-274

22. Harold, D., Abraham, R., Hollingworth, P., Sims, R., Gerrish, A., Hamshere, M. L., Pahwa, J. S., Moskvina, V., Dowzell, K., Williams, A., Jones, N., Thomas, C., Stretton, A., Morgan, A. R., Lovestone, S., Powell, J., Proitsi, P., Lupton, M. K., Brayne, C., Rubin- sztein, D. C., Gill, M., Lawlor, B., Lynch, A., Morgan, K., Brown, K. S., Passmore, P. A., Craig, D., McGuin- ness, B., Todd, S., Holmes, C., Mann, D., Smith, A. D., Love, S., Kehoe, P. G., Hardy, J., Mead, S., Fox, N., Rossor, M., Collinge, J., Maier, W., Jessen, F., Schürmann, B., van den Bussche, H., Heuser, I., Kornhu- ber, J., Wiltfang, J., Dichgans, M., Frölich, L., Hampel, H., Hüll, M., Rujescu, D., Goate, A. M., Kauwe, J. S., Cruchaga, C., Nowotny, P., Morris, J. C., Mayo, K., Sleegers, K., Bettens, K., Engelborghs, S., De Deyn, P. P., Van Broeckhoven, C., Livingston, G., Bass, N. J., Gurl- ing, H., McQuillin, A., Gwilliam, R., Deloukas, P., Al-Chalabi, A., Shaw, C. E., Tsolaki, M., Singleton, A. B., Guerreiro, R., Mühleisen, T. W., Nöthen, M. M., Moebus, S., Jöckel, K. H., Klopp, N., Wichmann, H. E., Carrasquillo, M. M., Pankratz, V. S., Younkin, S. G., Holmans, P. A., O'Donovan, M., Owen, M. J., and Williams, J. (2009). Genome-Wide Association Study identifies variants at CLU and PICALM associated with Alzheimer's disease. *Nat. Genet.* 41, 1088–1093.

23. Hollingworth, P., Harold, D., Sims, R., Gerrish, A., Lambert, J. C., Carrasquillo, M. M., Abraham, R., Hamshere, M. L., Pahwa, J. S., Moskvina, V., Dowzell, K., Jones, N., Stretton, A., Thomas, C., Richards, A., Ivanov, D., Widdowson, C., Chapman, J., Lovestone, S., Powell, J., Proitsi, P., Lupton, M. K., Brayne, C., Rubinsztein, D. C., Gill, M., Lawlor, B., Lynch, A., Brown, K. S., Passmore, P. A., Craig, D., McGuinness, B., Todd, S., Holmes, C., Mann, D., Smith, A. D., Beaumont, H., Warden, D., Wilcock, G., Love, S., Kehoe, P. G., Hooper, N. M., Vardy, E. R., Hardy, J., Mead, S., Fox, N. C., Rossor, M., Collinge, J., Maier, W., Jessen, F., Rüther, E., Schürmann, B., Heun, R., Kölsch, H., van den Bussche, H., Heuser, I., Kornhuber, J., Wiltfang, J., Dichgans, M., Frölich, L., Hampel, H., Gallacher, J., Hüll, M., Rujescu, D., Giegling, I., Goate, A. M., Kauwe, J. S., Cruchaga, C., Nowotny, P., Morris, J. C., Mayo, K., Sleegers, K., Bettens, K., Engelborghs, S., De Deyn, P. P., Van Broeckhoven, C., Livingston, G., Bass, N. J., Gurl- ing, H., McQuillin, A., Gwilliam, R., Deloukas, P., Al-Chalabi, A., Shaw, C. E., Tsolaki, M., Singleton, A. B., Guerreiro, R., Mühleisen, T. W., Nöthen, M. M., Moebus, S.,Jöckel, K. H., Klopp, N., Wichmann, H. E., Pankratz, V. S., Sando, S. B., Aasly, J. O., Barcikowska, M., Wszolek, Z. K., Dickson, D. W., Graff-Radford, N. R., Petersen, R. C., Alzheimer's Disease Neuroimaging Initiative, van Duijn, C. M., Breteler, M. M., Ikram, M. A., DeStefano, A. L., Fitzpatrick, A. L., Lopez, O., Launer, L. J., Seshadri, S., CHARGE Consortium, Berr, C., Campion, D., Epelbaum, J., Dartigues, J. F., Tzou- rio, C., Alpérovitch, A., Lathrop, M., EADI1 consortium, Feulner, T. M., Friedrich, P., Riehle, C., Kraw- czak, M., Schreiber, S., Mayhaus, M., Nicolhaus, S., Wagenpfeil, S., Stein- berg, S., Stefansson, H., Stefansson, K., Snaedal, J., Björnsson, S., Jons- son, P. V., Chouraki, V., Genier-Boley, B., Hiltunen, M., Soininen, H., Com- barros, O., Zelenika, D., Delepine, M., Bullido, M. J., Pasquier, F., Mateo, I., Frank-Garcia, A., Porcellini, E., Hanon, O., Coto, E., Alvarez, V., Bosco, P., Siciliano, G., Mancuso, M., Panza, F., Solfrizzi, V., Nacmias, B., Sorbi, S., Bossù, P., Piccardi, P., Arosio, B., Annoni, G., Seripa, D., Pilotto, A., Scarpini, E., Galimberti, D., Brice, A., Hannequin, D., Licastro, F., Jones, L., Holmans, P. A., Jon- sson. T., Riemenschneider, M., Mor- gan, K., Younkin, S. G., Owen, M. J., O'Donovan, M., Amouyel, P., and Williams, J. (2011b). Common vari- ants at ABCA7, MS4A6A/MS4A4E, EPHA1, CD33 and CD2AP are asso- ciated with Alzheimer's disease. *Nat. Genet.* 43, 429–435.

24. Hoozemans JJ, van Haastert ES, Nijholt DA, Rozemuller AJ, Eikelenboom P, Scheper W (2009) The unfolded protein response is activated in pretangle neurons in Alzheimer's disease hippocampus. The American Journal of Pathology, 4: 1241-1251

25. Hoozemans JJ, Veerhuis R, Van Haastert ES, Rozemuller JM, Baas F, Eikelenboom P, Scheper W (2005) The unfoled protein response is activated in Alzheimer's disease. Acta Nerupathol, 110: 165-172

26. Hong L, Huang HC, Jiang ZF (2014) The relationship between amyloid-beta and the ubiquitin-proteasome system in Alzheimer's disease. Neurological Research 3: 276-282

27. Hope AD, de Silva R, Fischer DF, Hol EM, van leeuwen FW, Lees AJ (2003) Alzheimer's associated variant ubiquitin causes inhibition of the 26S proteasome and chaperone expression. J. Neurochem, 86: 394-404

28. Ingelsson M (2004) Early Abeta accumulation and progressive synaptic loss, gliosis, and tangle formation in AD brain. Neurology 62, 925-931.

29. Jee SW, Cho JS, Oh JH, Shim SB, Hwang DY, Lee SH, Song YS, Kim YK (2005) cDNA microarray-based analysis of differen- tially expressed genes in transgenic brains expressing NSE- controlled APPsw. Int J Mol Med 16:547–552

30. Keck S, Nitsch R, Grune T, Ullrich O (2003) Proteasome inhibition by paired helical filament-tau in brains of patients with Alzheimer's disease. J. Neurochem, 85: 115-122

31. Keller JN, Hanni KB, Markesbery WR (2000) Impaired proteasome function in Alzheimer's disease. J. Neurochem, 75: 436-439.

32. Kozutsumi Y, Segal M, Normington K, Gething MJ, Sambrook J (1988) The presence of malfolded proteins in the endoplasmic reticulum signals the induction of glucose-regulated proteins. Nature, 332: 462-464

33. Lambert, J. C., Zelenika, D., Hiltunen, M., Chouraki, V., Combarros, O., Bullido, M. J., Tognoni, G., Fiévet, N., Boland, A., Arosio, B., Coto, E., Del Zompo, M., Mateo, I., Frank- Garcia, A., Helisalmi, S., Porcellini, E., Pilotto, A., Forti, P., Ferri, R., Delepine, M., Scarpini, E., Sicil- iano, G., Solfrizzi, V., Sorbi, S., Spal- letta, G., Ravaglia, G., Valdivieso, F., Alvarez, V., Bosco, P., Mancuso, M., Panza, F., Nacmias, B., Bossù, P., Piccardi, P., Annoni, G., Seripa, D., Galimberti, D., Licastro, F., Lath- rop, M., Soininen, H., and Amouyel, P. (2011). Evidence of the associ-

ation of BIN1 and PICALM with the AD risk in contrasting Euro- pean populations. *Neurobiol. Aging*32, 756.e11–756.e15.

34. Lopez OL (2011) The Growing Burden of Alzheimer's disease. AJMC 17: S339

35. Lopez SM, Pasquini L, Besio MM, Pasquini JM, Soto E (2003) Relationship between beta-amyloid degradation and the 26*S* proteasome in neural cells. Exp Neurol. 180: 131-43

36. Liang WS, Dunckley T, Beach TG, Grover A, Mastroeni D, Ramsey K, Caselli RJ, Kukull WA, McKeel D, Morris JC, Hulette CM, Schmechel D, Reiman EM, Rogers J, Stephan DA (2008) Altered neuronal gene expression in brain regions differentially affected by Alzheimer's disease: a reference data set. Physiol Genomics 33: 240-256

37. Mark RE (2012) Microglia in Alzheimer's Brain: A Neuropathological Perspective. International Journal of Alzheimer's Disease 10: 165021

38. Masters CL, Multhaup G, Simms G, Pottgiesser J, Martins RN, Beyreuther K (1985) Neuronal origin of a cerebral amyloid: neurofibrillary tangles of Alzheimer's disease contain the same protein as the amyloid of plaque cores and blood vessels. EMBO J 4(11): 2757-2763

39. Molsa PK, Marttila RJ, Rinne UK (1986) Survival and cause of death in Alzheimer's disease and multi-infarct dementia. Acta Neurol Scand, 74:103-7

40. Meinerst S, Heyken D, WalleR a, Ludwig A, Stangl K, Kloetzel PM, Krugers E (2003) Inhibition of proteasome activity induces concerted expression of proteasome genes and de novo formation of mammalian proteasomes. J. Biochem, 24: 21517-21525

41. Mortazavi A, Williams BA, McCue K, Schaeffer L, Wold B (2008) Mapping and quantifying mammalian transcriptomes by RNA-Seq. Nature 5, 621-628.

42. Nagy Z, Jobst KA, Esiri MM, Morris JH, King EM, MacDonald B, Litchfield S, Barnetson L, Smith AD (1996) Hippocampal pathology reflects memory deficit and brain imaging measurements in Alzheimer's Disease: clinicopathologic correlations using three sets of pathologic diagnostic criteria. Dementia 7, 76-81.

43. Oddo S, Caccamo A, Shepherd JD, Murphy MP, Golde TE, Kayed R, Mether- ate R, Mattson MP, Akbari Y, LaFerla FM (2003) Triple-transgenic model of Alzheimer's disease with plaques and tangles: intracellular Abeta and synaptic dysfunction. Neuron 39:409 – 421. CrossRef Medline

44. Perl DP (2010) Neuropathology of Alzheimer's disease. Mt Sinai J Med 77: 32-42

45. Pfaffl MW, Hageleit M (2001) Validities of mRNA quantification using recombinant RNA and recombinant DNA external calibration curves in real-time RT-PCR. Biotechnology letters 23: 275-282.

46. Reddy PH, McWeeney S, Park BS, Manczak M, Gutala RV, Partovi D, Jung Y, Yau V, Searles R, Mori M, Quinn J (2004) Gene expression profiles of transcripts in amyloid precursor protein transgenic mice: up-regulation of mitochondrial metabolism and apoptotic genes is an early cellular change in Alzheimer's disease. Hum Mol Genet 13:1225–1240

47. Reddy PH (2011) Abnormal tau, mitochondrial dysfunction, impaired axonal transport of mitochondria, and synaptic deprivation in Alzheimer's disease. Brain Res 1415: 136-148

48. Ricciarelli R, d'Abramo C, Massone S, Marinari U, Pronzato M, Tabaton M (2004) Microarray Analysis in Alzheimer's disease and normal aging. IUBMB Life 56: 349-354

49. Selkoe DJ (2001) Alzheimer's disease: genes, proteins, and therapy. Physiol Rev 81: 741-766

50. Sheng JG, Mark RE, Griffin WST (1997) Glia-neuronal interactions in alzheimer's disease: progressive association of il-1α+microglia and s100β+astrocytes with neurogibrillary tangle stages. Journal of Neruopathology and Experimental Neurology 56: 285-290.

51. Sultan M, Schulz MG, Richard H, Magen A, Klingrenhoff A, et al. (2008) A global view of gene activity and alternative splicing by deep sequencing of the human transcriptome. Science 321: 956-960

52. Sutherland GT, Janitz M, Kril JJ (2011) Understanding the pathogenesis of Alzheimer's disesase: will RNA-seq realize the promise of transcriptomics? Journal of Neurochemistry, 116: 937-946

53. Tang F, Barbacioru C, Wang Y, Nordman E, Lee C, Xu N, Wang X, Bodeau J, T BB, Siddiqui A, Lao K, Surani MA (2009) mRNA-Seq whole-transcriptome analysis of a single cell. Nature Methods 6: 377-382

54. Terry RD (1963) The fine structure of neurofibrillary tangles in Alzheimer's disease. J Neuropathol Exp 22: 629-642

55. Twine NA, Janitz K, Wilkins MR, Janitz M (2011) Whole Transcriptome Sequencing Reveals Gene Expression and Splicing Differences in Brain Regions Affected by Alzheimer's disease. PLoS ONE 6(1)

56. Van Leeuwen FW, Fischer DF, Kamel D, Slujis JA, Sonnemans MA, Benne R, Swaab DF, Salehi A, Hol EM (2000) Molecular misreading: a new type of transcript mutation expressed during aging. Neurobiol. Aging, 21:879-891

57. Van Leeuwen FW, de Klejin DP, van den Hurk HH, Neubauer A, Sonnemans MA, Slujis JA, Koycus S, Ramdjielal RD, Salehi A, Martens GJ et al (1998) Frameshift mutants of beta amyloid precursor protein and ubiquitin-B in Alzheimer's and Down patients. Science, 279: 242-247

58. Wilson CA, Doms RW, Lee V (1999) Intracellular APP Processing and A[Beta] Production in Alzheimer's disease. J Neuropahol Exp 58: 742-748

59. Wong PC, Cai H, Borchelt DR, Price DL (2002) Genetically engineered mouse models of neurodegenerative diseases. Nature neuroscience 5: 633-639

60. Watanabe T, Hikichi Y, Willuweit A, Shintani Y, Horiguchi T (2012) FBL2 regulates amyloid precursor protein (APP) metabolism by promoting ubiquination-dependent APP degradation and inhibition of APP endocytosis. J Neurosci, 19:67

61. Wang Z, Gerstein M, Snyder M (2009) RNA-seq: a revolutionary tool for transcriptomics. Nature Reviews Genetics 10: 57-63

62. Zhao X, Yang J (2010) Amyloid-beta peptide is a substrate of the human 20S proteasome. ACS chem Neurosci. 1:655-60